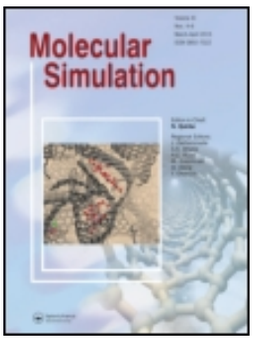

Molecular Simulation

ISSN: 0892-7022 (Print) 1029-0435 (Online) Journal homepage: http://www.tandfonline.com/loi/gmos20

A versatile modelling approach to determine the hydrophobicity of peptides at the atomic level

Myhuong T. Nguyen, Alan L. Chaffee, Reinhard I. Boysen, Dan V. Nicolau & Milton T.W. Hearn

To cite this article: Myhuong T. Nguyen, Alan L. Chaffee, Reinhard I. Boysen, Dan V. Nicolau & Milton T.W. Hearn (2016) A versatile modelling approach to determine the hydrophobicity of peptides at the atomic level, Molecular Simulation, 42:4, 257-269, DOI: 10.1080/08927022.2015.1038533

To link to this article: http://dx.doi.org/10.1080/08927022.2015.1038533

Published online: 03 Aug 2015.

Molecular Simulation, 2016
Vol. 42, No. 4, 257–269, http://dx.doi.org/10.1080/08927022.2015.1038533

Taylor & Francis
Taylor & Francis Group

A versatile modelling approach to determine the hydrophobicity of peptides at the atomic level

Myhuong T. Nguyen, Alan L. Chaffee, Reinhard I. Boysen, Dan V. Nicolau[1] and Milton T.W. Hearn*

Centre for Green Chemistry, School of Chemistry, Monash University, Melbourne, Vic 3800, Australia

(*Received 2 September 2014; final version received 2 April 2015*)

This study describes a versatile computational method to determine the hydrophobicity of small peptides at the atomic level. Free energies of transfer for individual atoms in peptide structures were derived, utilising two specifically defined parameters: (i) the water-excluding distance to define the dynamic interface between a peptide solute and its surrounding solvent and (ii) the corresponding hydrophobicity index as a relative measure for water occlusion/repulsion. The method was tested on a range of small peptide models (Ac-**X**-NH_2, G-**X**-G, Ac-WL-**X**-LL and Ac-GG-**X**-GG-NH_2) and several derivatives of these structures, whereby **X** was any of the 20 most common amino acids that naturally occur in polypeptides or proteins. The advantage of this new method lies in its versatility, ease to implement and capability to provide information on the hydrophobicity characteristics at the atomic level. The approach also encapsulates the impact of factors that influence these properties, but which have hitherto been difficult to accurately quantify, e.g. steric hindrance or proximity effects due to nearby polarised atoms. The method is not conditional on the knowledge of hydrophobicity parameters from the literature and does not require a sophisticated computer software/hardware to enable the atomic solvent-accessible surface areas or other hydrophobicity parameters to be *de novo* obtained.

Keywords: atomic hydrophobicity; peptides; free energy of transfer; hydrophobicity index; molecular dynamics

1. Introduction

At a physicochemical level, the hydrophobic effect is the tendency of a molecule to repel water, or alternately, it can be defined by a strong affinity of atoms/molecules towards each other resulting in an exclusion of water. Its impact is usually quantified in terms of different experimental techniques, such as octanol–water partition or contact angle measurements, or expressed in terms of relative hydrophobicity parameters or values. The concept has been widely used to rationalise the solubility of chemical and biological compounds and to elaborate the processes that govern numerous chemical and biological processes, e.g. molecular transport, distribution/partition, self-assembly, molecular recognition and the generation of supramolecular architectures.

Knowledge of how the hydrophobic effect and the associated hydrophobicity parameters are manifested thus aids elucidation of the behaviour of molecules of interest in various environments. Such information has been of special importance in the study of proteins, since it has been long recognised that there is a direct linkage between the interplay of hydrophobic effects, the intrinsic hydrophobicities of the different amino acids (AAs) in the primary structure, and the stability, folded status, binding propensities and bioactivity of a protein.[1–3] Similar considerations apply to the behaviour of small peptides in terms of their solvational properties, and ability to self-associate and form supramolecular structures. Consequently, the determination of the hydrophobicity of naturally occurring, proteinogenic AAs has been a subject of a wide range of experimental, theoretical and computational studies over several decades.[4–12] Numerous AA hydrophobicity scales have been derived; however, their values and utility vary greatly. Moreover, these scales are typically not atomistic, but rather have been generally based on AA compositional or fragment groupings.[6–9,12–19]

Hitherto, the derivation of the hydrophobicity of a small peptide or even a protein has commonly started with the selection from the scientific literature of hydrophobicity values for individual fragments, such as the AA side chains. These values are then adjusted to suit the specific application, mostly by summation of correction factors, to define the apparent hydrophobicity value of a fragment in a particular peptide sequence, i.e. by using a bottom-up approach. Such approaches experimentally have often been based on the use of the reversed-phase high-performance liquid chromatographic data derived with sets of peptide homologues and analogues.[3,6–8] The successful application of such methods is, however, conditional on inclusion of all factors influencing the hydrophobicity of the fragment. When the number of these factors and their possible combinations is taken into consideration, the result is an ever-expanding list of hydrophobicity databases and correction methodologies.

Alternatively, solvent-accessible surface areas (ASAs) have been used to qualitatively anticipate properties related to molecular hydrophobicity.[7,20–22] Although

*Corresponding author. Email: milton.hearn@monash.edu

ASAs of intact peptides and proteins can be calculated by a variety of molecular visualisation programs, such as VMD [http://www.ks.uiuc.edu/Development/Download/download.cgi?PackageName=VMD], POPs [http://mathbio.nimr.mrc.ac.uk/wiki/POPS] or SURFACE [http://wiki.c2b2.columbia.edu/honiglab_public/index.php/Software:SURFace_Algorithms], these methods cannot calculate ASAs for individual atoms in different solvational or conformational states in the molecule, which require more sophisticated atomistic hydrophobicity calculations.

The objectives of the current studies were thus to focus on the validation of an alternative approach to determine atomic hydrophobicities of AAs exemplified for small peptide structures, based on the molecular dynamic (MD) analysis of multiple statistically relevant dynamics frame trajectories related to the solvational and conformational preferences of individual atoms within the AA sequence of a set of small peptides. The approach described herein does not rely on the availability of any special calculations of parameters, such as hydrophobicity constants or solvent-ASAs, for individual atoms in the peptide of interest, or the need to access specialised databases. The approach employs modelling methods based on MDs to simulate the peptide–water system. The simulation data are then used to calculate the hydrophobicity index (HI) and the free energy of transfer for each individual atom in the structure. In developing this approach, we have used small molecules, including acetyl amino amides, tripeptides and pentapeptides, as exemplars to illustrate the basis of this computational approach and to validate the fundamental methodology of the investigation. Since all hydrophobicity data are obtained at an atomic level, this approach potentially provides a new avenue to gain insights into more complex processes and other peptide properties, as the results are gathered at atomic resolution. In particular, the method provides a detailed map of the hydrophobicity characteristics for all atoms in a peptide structure, thus underpinning a more comprehensive structural interpretation of the nature of the intra- and inter-molecular interactions involved in solvation or functionality – a task which has hitherto usually been achieved with much more sophisticated computer software/hardware facilities and extensive hydrophobicity databases.

2. Computational modelling procedures

2.1 Molecular models and methods

A series of AAs and small peptide molecules in the form of Ac-**X**-NH_2, G-**X**-G, Ac-GG-**X**-GG-NH_2 and Ac-WL-**X**-LL, and selected derivatives of these structures were constructed *in silico*, where **X** was any AA residue. Although only selected results are discussed in this paper, all 20 natural AAs were included in each set. The conformation of each peptide was modelled to be consistent with the protonation state of the side chain of its AA residues at pH 9.0. Under these conditions, the side chains of most of the AA residues within the chosen peptide sets will be uncharged, except for those of Asp, Glu, Arg and Lys, where the charge carried by the side chains of these AA residues will be (−), (−), (+) and (+), respectively. Aspartic acid was chosen as an exemplar AA for evaluation with this new methodology, since the carboxylic acid group of its side chain has a p$Ka = 3.90$ and thus this side chain will essentially be fully deprotonated at pH 9.0. Clearly, the described methodology has the capability to be extended to also encompass the effects of other pH conditions on the ionisation status of the AA side chains, i.e. at low pH such as pH 1.0 or at neutral pH 7.0, beside the selected pH 9.0 conditions.

The Materials Studio (MS, Materials Studio® Accelrys, Inc., San Diego, CA, USA) Amorphous Cell Construction module was used to build a periodic cubic cell of each single peptide molecule submerged in 600 water molecules. The solution density was set at 1 g cm^{-3}. Before the cell construction, a stable peptide configuration was achieved using the DISCOVER Energy Minimizer module Smart Minimizer, which is a combination of Steepest Descent, Conjugate gradient and Newton methods. The cell construction was followed by geometry optimisation leading to refined configurations. The peptide–water system was then equilibrated using the Smart Minimizer. The equilibrium properties of the system were sampled in an NVT ensemble using the DISCOVER Molecular Dynamics module. The COMPASS (Condensed-phase Optimized Molecular Potentials for Atomistic Simulation Studies) force field was used for both the energy minimisation (medium/fine level) and the MDs simulation. The COMPASS force field explicitly covers all AA functional groups and has been widely used for modelling and simulation of organic molecules and water as a solvent, including AAs [http://www.esi.umontreal.ca/accelrys/life/cerius46/compass].[23–25] MDs runs were carried out at 298 K (temperature thermostat Andersen) using a time step of 1 fs, and Ewald summation for handling long-range electrostatic and van der Waals interactions. A total simulation time of 400 ps was used for each MDs run. Data were collected at a frequency of 200 fs. In common with many other CPU-intensive investigations, a simulation time of 400 ps was chosen being a reasonable trade-off between the time available to complete the study and the computing capacity. It is sufficient for a bulky side chain of an AA residue, such as tryptophan or arginine, to completely rotate around a specific amide bond α-carbon atom of the peptide backbone of any host peptide structures used in the study. This procedure is similar to that described by Wimley et al. [17] although in this case these investigators used the Monte Carlo Method instead. The Wimley et al.

procedure was closely followed as their data were subsequently utilised for validation of our method. The mean square displacement was also calculated and analysed for the system without a peptide molecule, and with selected peptide molecules (up to 7 AA units), for the same simulation time scale, confirming that these systems were well established in the self-diffusion region. Root mean square deviation (RMSD) calculations were also performed to confirm that the peptide structures had reached stability within the simulation time period. The RMSD values were obtained according to

$$\mathrm{RMSD}(t) = \sqrt{\frac{1}{N}\sum_{i=1}^{N}\left|\mathbf{x}_{i(t)} - \mathbf{x}_{i(o)}\right|^2}, \quad (1)$$

where $\mathbf{x}_{i(o)}$ and $\mathbf{x}_{i(t)}$ are coordinates of peptide atoms, after removing the global translations and rotations, at time *0* and *t*, respectively [26,27] [http:/boscoh.com/code].

The chosen simulation time was comparable to that used for systems of a similar molecular size [28–30] and sufficient to ensure all mean values of the system trajectory to be statistically meaningful. These results, using this simulation time scale, are thus very consistent with theoretical predictions and work reported by other investigators for similar systems (as further discussed in Section 3).

The behaviour (trajectory) of the peptide molecule was observed (MS Visualizer®, San Diego, CA, USA) and also evaluated using a number of MS calculation tools. Radial distribution functions (RDFs) for AA atoms of interest and water oxygen atoms were calculated using MS RDF tools. The MS Discover hydrogen bond calculation tool was used to monitor the existence of hydrogen bonds with the selected peptide–water systems. A new program, called Monash-HPT, was developed specifically for this purpose to enable the calculation of hydrophobicity parameters for each peptide trajectory.

2.2 Water-excluding distance

The water-excluding distance (WED) is defined as the distance, *d*, of an AA atom from its nearest water oxygen,

$$d = \sqrt{(x_{\min} - x_{\mathrm{aa}})^2 + \left(y_{\min} - y_{\mathrm{aa}}\right)^2 + (z_{\min} - z_{\mathrm{aa}})^2}, \quad (2)$$

where *x*, *y* and *z* are the Cartesian coordinates of the atoms, the subscript min relates to the distance to the nearest water oxygen and the subscript aa relates to the atom of the amino acid. This quantity was calculated taking into account the periodic boundary conditions of the simulation system. For a trajectory, the WED was determined for each AA atom in the peptide for each frame in the trajectory, the water-excluding distance distribution (WEDD) was generated and a time-averaged WED for each AA atom was then calculated.

2.3 Hydrophobicity Index

In order to quantify the atomic hydrophobicity effect for AA atoms, we defined a new parameter, the HI, which is derived by applying the Boltzmann distribution law,[31] namely

$$\frac{N_j}{N} = \frac{\exp\left(\frac{-\varepsilon_j}{k_B T}\right)}{\sum_i \exp\left(\frac{-\varepsilon_i}{k_B T}\right)}, \quad (3)$$

to both the AA atom and a water molecule in the bulk, then dividing their ratio by a factor $k_B T$. The HI, therefore, is expressed as

$$\mathrm{HI} = -\ln\left(\frac{N_{\mathrm{aa}}}{N_{\mathrm{ww}}}\right). \quad (4)$$

In Equation (3), N_j is the number of particles that have the energy ε_j, N the total number of all particles i with the respective energy ε_i in the system, k_B the Boltzmann constant and T the absolute temperature. In Equation (4), N_{aa} is the number of water molecules at the AA atom-water interface and N_{ww} the number of water molecules surrounding other water molecules in the bulk at the same distance, as specified by the WEDD of the AA residue.

To calculate the atom's HI, an interface thickness for the whole AA residue was defined by the minimum and maximum WED values of all individual atomic WEDs. The HI reflects the degree of water occlusion/repulsion as a result of molecular geometry, potential and H-bonding energies of the atom in comparison with other atoms in the residue. Higher HI values correspond to a greater proportion of atoms occluded from the surrounding water. To calculate this value, a number of water molecules in the bulk were randomly selected and their number-averaged values as well as time-averaged values were used.

2.4 Atomic free energy of transfer, ΔG^{tr}_{aa}

Utilising the concept of hydrophobicity index (HI), but for individual atom interface thickness, the hydrophobic free energy of each AA atom can be expressed as follows:

$$\Delta E_{\mathrm{aa}} = -\mathrm{RT}\frac{\rho_d}{\rho}\ln\left(\frac{N_{\mathrm{aa}}}{N_{\mathrm{ww}}}\right), \quad (5)$$

where R is the gas constant, and ρ_d and ρ are particle densities at the atom interface and of the system, respectively. The atomic free energy of transfer ($\Delta G^{\mathrm{tr}}_{\mathrm{aa}}$) is the sum of the hydrophobic free energy defined in Equation (5) and the H-bonding energy, if that occurs

during the simulation. We consider that an H-bond is formed when the distance between the atom and a water molecule is ≤ 2.5 Å. The value employed for the H-bonding energy for a single H-bond was 1.6 kcal mol^{-1} as reported by Pace et al. [32] Thus, ΔG^{tr}_{aa} can be expressed as

$$\Delta G^{tr}_{aa} = \Delta E_{aa} + 1.6 P_{H-bond}, \quad (6)$$

where $P_{H\text{-bond}}$ is the probability of H-bonding occurrence during the simulation.

The molecular free energy of transfer (ΔG^{tr}_{mol}) is then obtained by summation of the atomic free energies (ΔG^{tr}_{aa}) of all atoms in the residue. This calculation of ΔG^{tr}_{aa} is basically equivalent to the change in energy by replacing a water molecule with an AA atom. More rigorous algorithms that include other factors influencing H-bonding, such as bond angle, could be used to detect H-bonds and calculate their energy. However, a distance ≤ 2.5 Å and the energy criterion of 1.6 kcal mol^{-1} for hydrogen bonds were found sufficient for the systems under study.

3. Results and discussion

In the current investigations addressing the hydrophobicity of small peptides at the atomic level, results from the application of the COMPASS force field were first validated against data reported in the literature. These initial investigations focused on the use of the RDF to quantify hydrophobicity at the atomic level and revealed several shortcomings of the RDF approach (Section 3.2). Nevertheless, these RDF studies enabled useful insights to be garnered, which enabled boundary conditions to be delineated and used in the development of a more practical method to quantify atomic hydrophobicity through the use of the WED and the atomic hydrophobicity free energy of transfer, ΔG^{tr}_{aa}.

3.1 Validation of the application of the force field COMPASS

The COMPASS force field was first tested on a dynamics modelling system using a box of 600 water molecules at 298 K. The RDFs so obtained from this simulation for this model water system agreed well with those published by Lee and Tuckerman [33] as shown in Figure 1. These earlier studies of Lee and Tuckerman were based on a CPAIMD/DVR (Car-Parrinello *ab initio* MDs/discrete variable representation) simulation, which was carried out under slightly different conditions (e.g., employed 32 water molecules at 300 K), and produced an O—O distance peak at 2.77 Å, which is within the range of water oxygen distance obtained experimentally, e.g., 2.73 Å from neutron scattering (at 298 K),[34] or 2.8 Å from X-ray

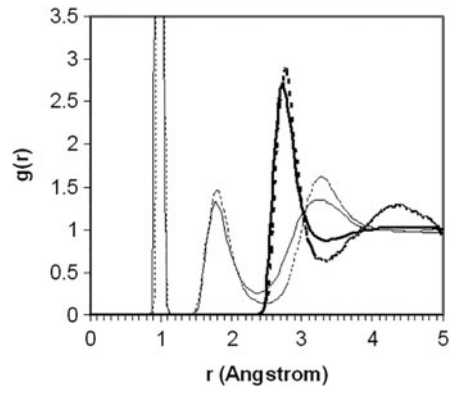

Figure 1. Comparison of RDFs for water structure obtained in this current work (solid line) using force field COMPASS, and that obtained by Lee et al. (broken line).[33] Fine lines are for O—H, and strong lines are for O—O. Peak position for O—O was 2.73 Å in this work, and 2.77 Å in Lee et al. [33]

scattering measurements (at 300 K).[35] The O—O distance obtained as part of our current work using the COMPASS force field was 2.73 Å. RMSD plots of the trajectories showed that the peptide systems had reached stability within the simulation time period with some structures fluctuating between various metastable configurations (usually two were dominant) over the duration of the simulation. These results, thus, agree well with experimental and modelling data published in the literature.

3.2 RDF and atomic hydrophobicity

RDFs have been widely used for obtaining hydrophobicity information. They have been used to deduce the structure of water molecules around an atom or a group of atoms of interest, which, in turn, has been assumed to reflect the interaction between the atom of interest and water. The first hydration shell of an atom and its coordination number can be identified from an RDF curve.[28,29] Subsequently, information on how an AA residue is exposed to and interacts with water under dynamic conditions at a specific temperature can then be assessed. [36,37]

In principle, the use of RDFs for individual atoms in an AA residue, i.e. each AA atom, with respect to the oxygen atoms of water, enables the water structure around each AA atom to be profiled and the microenvironment around the atom to be characterised in terms of its hydrophobic or hydrophilic character. For instance, a comparison of the RDF curves for the aspartic acid (Asp) atoms in Ac-**D**-NH_2 and Ac-WL-**D**-LL shows that the Asp residue (including the peptide amide bond atoms) in the pentapeptide Ac-WL-**D**-LL is slightly more hydrophobic when compared with this same residue in the structure Ac-**D**-NH_2. This outcome is due to the higher probability that

water molecules will be excluded to a greater distance from the backbone atoms (Figure 2). Interestingly, the RDF approach predicts that atoms in the side chain of this Asp residue exhibit a very similar hydrophobic behaviour for both structures. Moreover, the hydrophobicity of the Asp atoms also changes when the Asp moiety is located at a different position in the sequence of the peptide, as evident from the comparison between Ac-**D**-GGGG-NH_2 and Ac-GG-**D**-GG-NH_2 (Figure 3). In this case, the difference in hydrophobicity is more distinct for the Asp

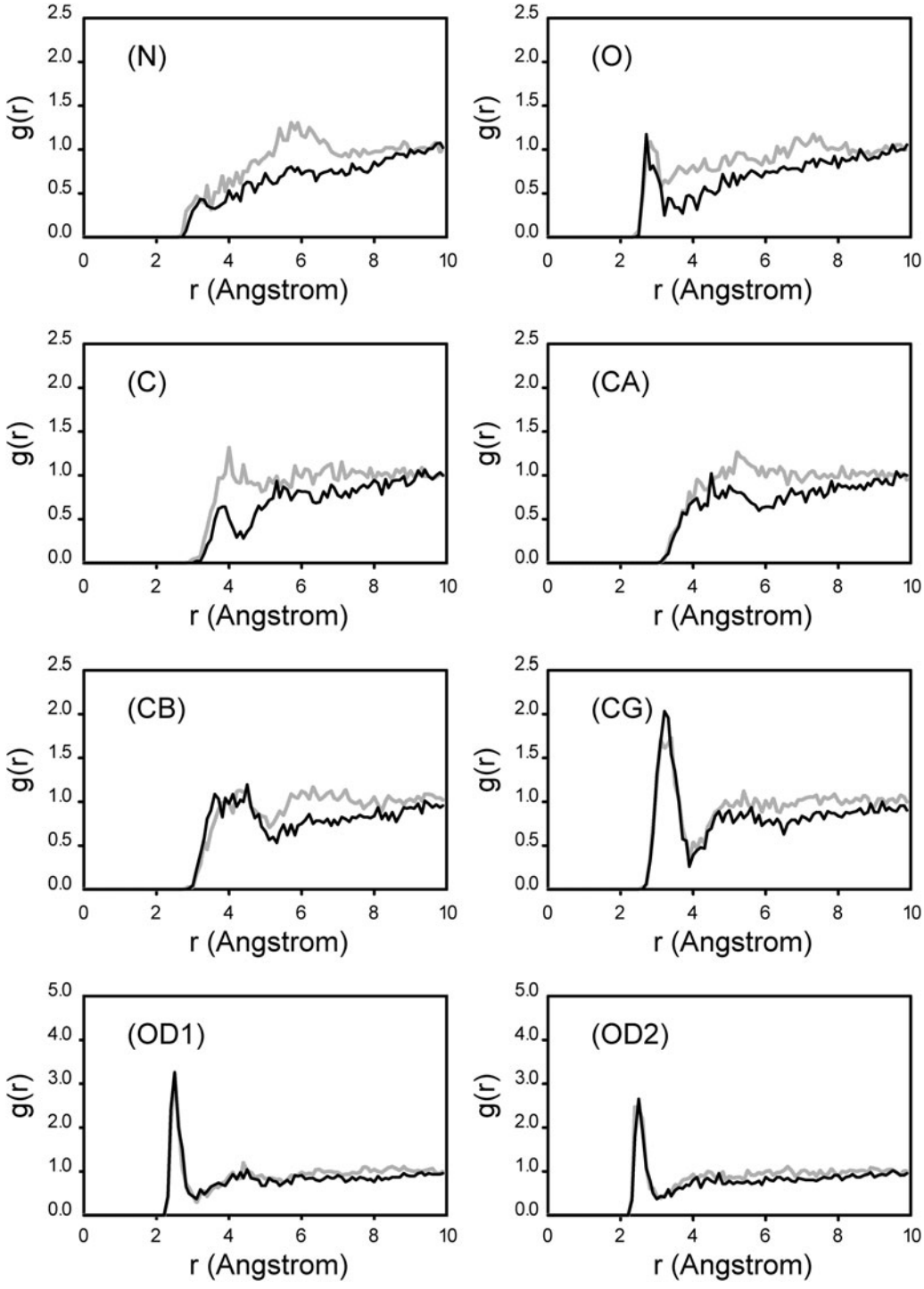

Figure 2. RDFs with respect to water oxygen atoms for Asp atoms in Ac-**D**-NH_2 (grey) and Ac-WL-**D**-LL-NH_2 (black) structures showing that the backbone Asp atoms in the latter structure are more hydrophobic, whereas the hydrophobicity of atoms in the side chain are similar in the two structures.

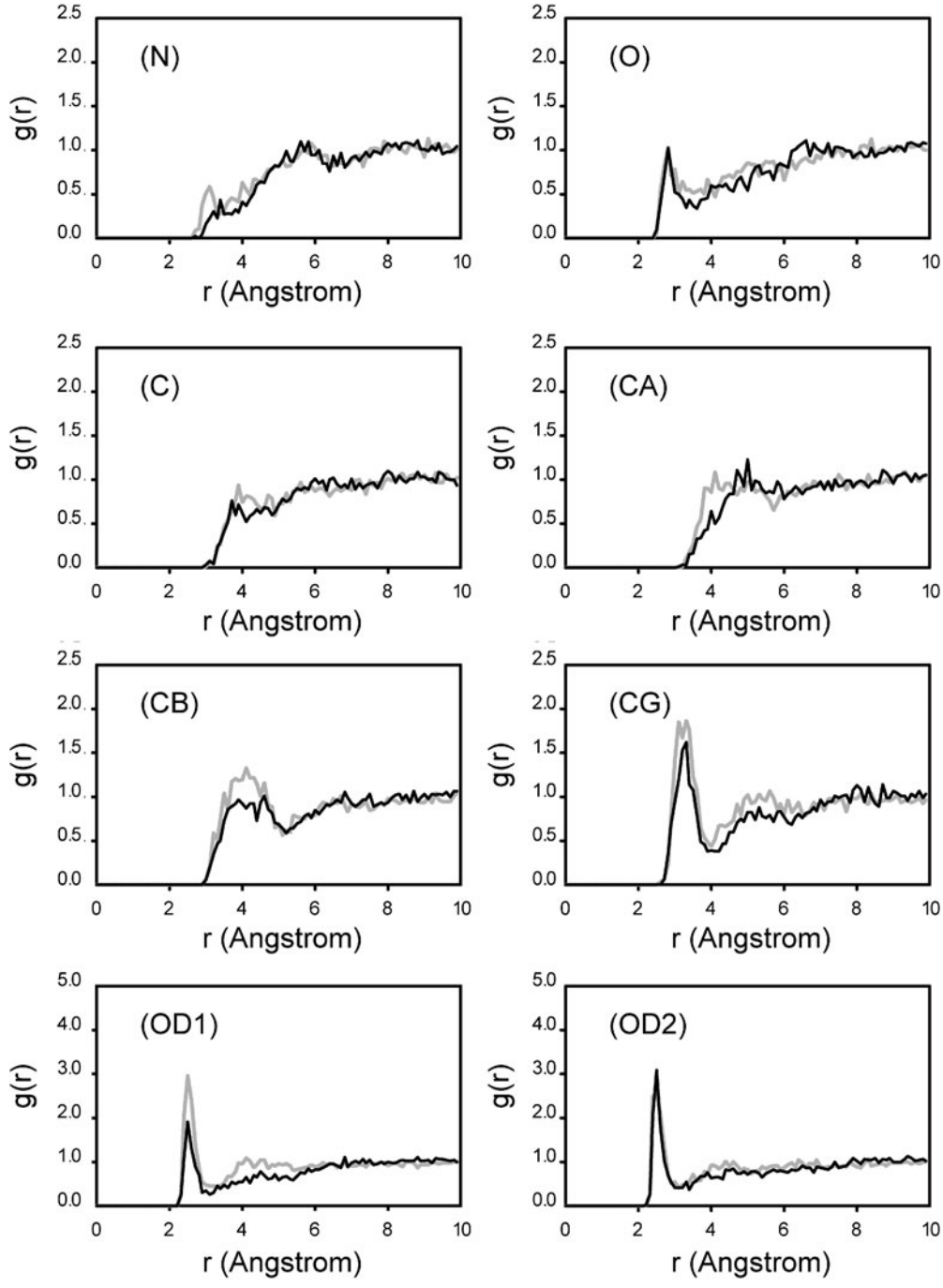

Figure 3. RDFs with respect to water oxygen atoms for Asp atoms in Ac-GG-**D**-GG-NH_2 (grey) and Ac-**D**-GGGG-NH_2 (black) showing that the side chain atoms in the latter structure are more hydrophobic, whereas the hydrophobicity of the backbone atoms of the two structures are similar.

side chain atoms. A change in hydrophobicity of the Asp atoms was also observed for the comparison between Ac-**D**-NH_2 and Ac-GG-**D**-GG-NH_2 (data not shown).

These examples demonstrate that the hydrophobicities of individual AA atoms change with different peptide structures as well as when the AA is in different sequence positions in the peptide backbone. This finding is not unexpected since water occlusion has an organisational dependency. Although not reported in the prior work, it is apparent from the current study, e.g. from a comparison between Ac-**D**-NH_2 and Ac-WL-**D**-LL (as well as the other peptide sets), that corrections to the values of the solvent-ASA of the AA atoms are needed to account for this organisational occlusion of solvent from an AA by

adjacent residues if the more traditionally derived hydrophobicities of individual AA atoms are to be used as derived, for example by the method of Wimley et al. [17] from the solvation energies of AA side chains. It can also be noted that, although this proposed WEDD method did not require calculations of atomic ASA, water-occlusion effects are reflected in experimental results.

Generally, the magnitude of changes in atomic hydrophobicity due to the position of an AA in the primary structure of a peptide, as evident from the comparisons, Ac-**D**-GGGG-NH_2 versus Ac-GG-**D**-GG-NH_2, or Ac-**D**-NH_2 versus Ac-GG-**D**-GG-NH_2, has not been addressed in prior hydrophobicity calculations, despite the fact that a wide range of influencing factors on AA hydrophobicity have to be considered. Moreover, it would be a very difficult and time-consuming task when bottom-up approaches are used to include all of these factors in the calculation of hydrophobicity, considering the great number of possible combinations that are involved. Similarly, the use of RDF for studying atomic hydrophobicity of larger peptides or proteins will be even more limited, due to the fact that identification of the first hydration shell and the hydrophobicity analysis for each atom in a large peptide or protein structure from their RDFs would be very time consuming due to their molecular size. Therefore, the use of RDF for quantifying atomic hydrophobicity does not represent an optimal, practical option.

3.3 The WED: a versatile approach to quantify atomic hydrophobicity

To simplify determination and quantification of atomic hydrophobicities, we have employed a new parameter, the WED,[30,38] based on the concept that an interface region can be defined between the atoms of an AA, present in a peptide, and water. The water molecules in this interface are then used to quantitatively assess the atomic free energy of transfer and the HI for each atom of the AA residue (include all of the backbone and chain residue atoms) of interest.

WED is defined as the shortest distance between the AA atom and its surrounding water oxygen atoms (Section 2.2). This distance is determined for every frame of the MDs trajectory. From this information, a WED distribution (WEDD) can be created (Figure 4). By extending the concept of hydrophobicity potential, introduced by Fauchère et al.,[39] and later utilised by Abraham and Kellogg in the HINT (hydrophobic interactions) program, [16,40] our studies have shown that the WED value identifies the position where an atom has its greatest apparent hydrophobicity potential. This distance varies during a MDs computational experiment, since it takes into account the change in the conformations of the residue and the host peptide backbone due to their interactions with water and with each other atom. The width of this WEDD therefore defines the thickness of the interface region, within which the AA atom exhibits a maximum hydrophobicity potential in that particular peptide structure.

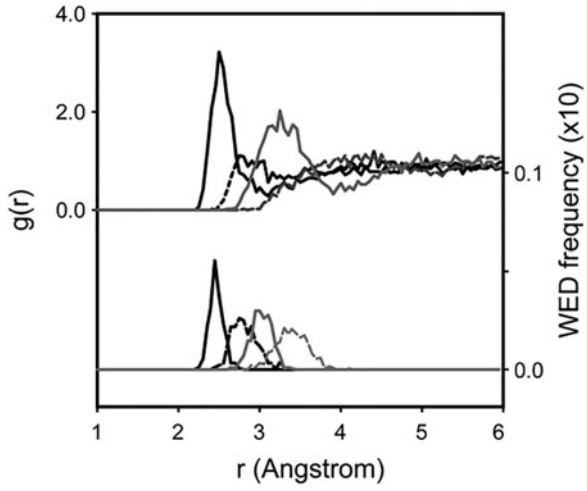

Figure 4. RDFs with respect to water oxygen atoms (upper panel) and WED frequency (lower panel) for selected Asp atoms in Ac-**D**-NH_2 showing that the two quantities have the same starting positions and relative peak position order. While the WEDD curves provide distinct start and end points, determination of the start and end points for the first peak in RDFs (the first hydration shell) is not straightforward. The WEDD curves are normalised and scaled up by 10 times for better visualisation. In both RDF and WEDD curves, black solid lines denote carboxyl oxygen atom (OD), black dashed lines carbonyl oxygen (O), grey solid lines carboxyl carbon (CG) and grey dashed lines CB atom.

Despite their differences in definition and physical meaning, the RDF and the WEDD have some characteristics in common. As shown in Figure 4, the WEDDs for Asp atoms have minimum *r*-values and the peak relative position order that are similar to the RDFs of the same atoms. The advantage of the WEDD is that it can be easily derived to define the interface region for any AA atom, while it can be difficult to identify the first hydration shell for some AA atoms, especially the hydrophobic ones, from their RDF curves.

It is also noteworthy that the interface defined by WED is not the same as the solvent-ASA used in other hydrophobicity calculations. ASA is generated by rolling a solvent molecule probe onto the solute molecular surface. The ASA calculation is based on the assumption that both the AA atom and the water probe are hard spheres (using their van der Waals radii).[41–43] The ASA is normally calculated from a single molecular conformation, but the WED is a result of dynamic interactions between the atom and water, which involve a range of factors such as charge status, influence of neighbouring groups, steric effects, electrostatic potential and H-bonding energy.

Table 1. Mean free energy of transfer (kcal mol^{-1}) calculated by this work for 20 natural AA side chain residues in series Ac-**X**-NH_2.

AA (1 letter code)	This work	Fauchère et al. [7] 0.65[a], 0.67[b]	Wimley et al. [17] 0.95[a], 0.81[b]	Eisenberg et al. [15] 0.64[a], 0.72[b]	Wilce et al. [8] 0.66[a], 0.56[b]
A	0.15	0.42	0.65	0.55	0.06
C	0.41	1.34	1.17	1.4	0.49
D	−1.83	−1.05	−2.49	−1.2	−0.20
E	−1.72	−0.87	−2.48	−0.76	−0.10
F	2.69	2.44	2.86	2.6	4.80
G	0.00	0.00	0.00	0.00	0.21
H	*	0.18	−1.18	0.25	−2.24
H^o	1.99	*	1.04	*	*
I	1.27	2.46	2.27	2.1	3.48
K	0.77	−1.35	−1.65	−0.78	−1.62
L	1.12	2.32	2.40	2	3.50
M	1.07	1.68	1.82	1.6	0.21
N	1.05	−0.82	0.30	−0.51	0.25
P(cis)/(trans)	0.79/0.95	0.98	1.01	1.5	0.71
Q	1.50	−0.3	0.38	−0.29	0.31
R	*	−1.37	−0.66	−2	−0.85
S	0.58	−0.05	0.69	−0.09	−0.62
T	0.78	0.35	0.90	0.58	0.65
V	0.74	1.66	1.61	1.6	1.59
W	4.01	3.07	3.24	2.7	2.29
Y	2.91	1.31	1.86	1.7	1.89

Notes: Comparison with the values reported in the literature.
*Indicates data are not available.
[a] The slope of the correlation line.
[b] The correlation coefficient.

3.4 Relationship between WED and atomic hydrophobicity free energy of transfer, ΔG^{tr}_{aa}

The atomic hydrophobicity free energy of transfer, ΔG^{tr}_{aa}, calculated in this current work relates to the energy difference generated when a water oxygen atom in the system is replaced with another atom of interest (see Section 2.4). Therefore, the derived atomic hydrophobicity free energies have the same significance as the free energies of transfer, well defined in the literature, [7,14,17,29,44] from experimental liquid partition data. To test this hypothesis, the free energies of 20 natural AAs in the series Ac-**X**-NH_2 were calculated (Table 1). The results for Arg and His were not included because it was found that the positive charge in the Arg and His side chains were not adequately represented by the COMPASS force field.

More generally, the simulation results obtained for the various AA atoms utilising this new approach agree well with experimental data reported for the same structure series (Ac-**X**-NH_2) [7] with the closest agreement found with those reported by Wimley et al.,[17] with the slope of the correlation line being almost unity, 0.95 ± 0.16 (Figure 5). Our hydrophobicity values (ΔG^{tr}_{aa}) also increase in the same general order as observed by clustering the AAs by group, as reported by both Fauchère et al. [7] and Wimley et al. [17] Specifically, for the non-polar AA residues, the hydrophobicity increases in the order of Ala < Cys < Val < Met < Leu < Phe < Trp, whereas for the hydrophilic AA residues, the values increase in the order of Asp < Glu < Lys < Asn < Gln < Tyr. It can also be noted that the literature data included in Table 1 were obtained using different host peptide structures on the assumption that these AA residues have the same exposure to water environment as their corresponding residues in the series Ac-**X**-NH_2. The excellent agreement

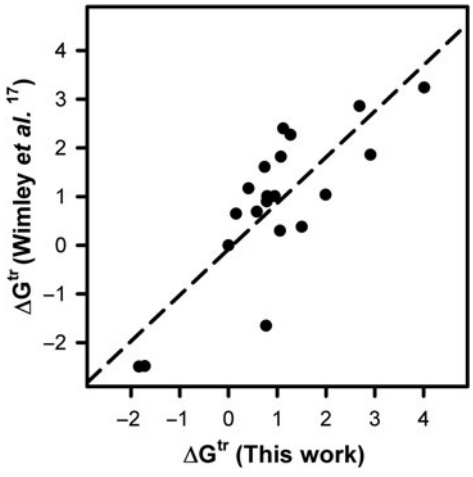

Figure 5. Correlation of free energy of transfer, ΔG^{tr}_{aa} (kcal mol^{-1}), for 20 natural AA side chain residues calculated by this current work and those obtained by Wimley et al. [17] showing that the two sets of data have similar magnitudes and are closely correlated ($r^2 = 0.81$).

for the trends in the ΔG_{aa}^{tr} values obtained in the current study with literature precedents validates the proposed approach as a reliable tool to obtain atomic free energy of transfer (ΔG_{aa}^{tr}) values for individual atoms in a peptide structure.

To further illustrate the capability of this new WED/ΔG_{aa}^{tr}-based method to differentiate factors that influence atomic hydrophobicity, the atomic free energy of transfer was determined for the Asp atoms in 11 different host peptide structures. The results of these studies are given in Table 2. From these results, the impact on the atomic hydrophobicities of the Asp residue in different environments, such as the position of the residue in the host peptide, the types of neighbouring residues and the host peptide structure, could be determined. For example, it was found that the effect of the amino group NH_2 (located at the C-terminal amide group) on the hydrophobicity of Asp side chain decreases with an increase in the number of Gly units between the amide group and the Asp residue. The plot of the free energy of transfer, ΔG_{aa}^{tr}, of the Asp side chain atoms versus the number of Gly spacers produced a hydrophobic increment of 0.24 kcal mol^{-1} per Gly unit (Figure 6) with the effect diminishing after 4 Gly units. On the other hand, the effect of an increasing number of the Gly units on both sides of Asp simultaneously did not follow this trend. The free energy of transfer, ΔG_{aa}^{tr}, values obtained for the Asp residue in WL-**D**-LL, Ac-**D**-NH_2 and Ac-GG-**D**-GG-NH_2 were generally consistent with their RDF values discussed earlier.

The influence of the hydrophobic behaviour of an atom can be further refined when the HI is included. Columns 2, 3 and 4 in Table 3 list the HI values for Asp atoms in Ac-**D**-NH_2 (1), Ac-WL-**D**-LL (2) and Ac-GG-**D**-GG-NH_2 (3), illustrating the steric environment for Asp atoms in each host structure. Higher HI values for the backbone atoms are due to the atom being shielded from water by adjacent groups (Ac-**D**-NH_2, Figure 7(a)), or neighbouring residues (Ac-WL-**D**-LL, Figure 7(b)), or by the two Gly arms of the host peptide backbone (Ac-GG-**D**-GG-NH_2, Figure 7(c)).

The values of the HI and atomic free energy of transfer for selected AAs in the series Ac-GG-**X**-GG-NH_2 are

Table 2. Free energy of transfer (kcal mol^{-1}) for the Asp individual atoms, its whole residue, back bone, side chain and the carboxyl group, and H-bonding energy in 11 host peptide structures.

Atom name	Ac-**D**-NH_2	Ac-**D**-G-NH_2	Ac-**D**-GG-NH_2	Ac-**D**-GGG-NH_2	Ac-**D**-GGGG-NH_2	Ac-**D**-GGGGG-NH_2
N	0.505	0.543	0.606	0.551	0.651	0.614
O	0.350 (−0.006)	0.483 (−0.008)	0.522 (−0.008)	0.517 (−0.002)	0.576 (−0.007)	0.594 (−0.008)
C	0.234	0.361	0.504	0.446	0.505	0.512
CA	0.369	0.274	0.285	0.342	0.365	0.422
CB	0.294	0.281	0.236	0.252	0.323	0.351
CG	0.151	0.206	0.227	0.218	0.244	0.310
OD1	−1.195 (−1.065)	−0.916 (−1.020)	−0.947 (−1.033)	−0.781 (−1.012)	−0.396 (−0.724)	−0.533 (−0.945)
OD2	−1.080 (−1.065)	−0.901 (−1.022)	−0.950 (−1.038)	−0.822 (−1.054)	−1.020 (−1.098)	−0.909 (−1.030)
Whole residue	−0.372	0.331	0.483	0.724	1.349	1.361
Backbone	1.458	1.661	1.917	1.857	2.098	2.142
Side chain	−1.830	−1.330	−1.434	−1.132	−0.749	−0.781
—COO^- group	−2.124	−1.610	−1.670	−1.385	−1.072	−1.132
H-bond	−2.130	−2.042	−2.071	−2.066	−1.822	−1.974

Atom Name	Ac-G-**D**-G-NH_2	Ac-GG-**D**-GG-NH_2	Ac-GGG-**D**-GGG-NH_2	Ac-GG-**D**-LG-NH_2	Ac-WL-**D**-LL
N	0.505	0.649	0.606	0.659	0.589
O	0.389 (−0.006)	0.494 (−0.010)	0.506 (−0.013)	0.609 (−0.006)	0.618 (−0.008)
C	0.362	0.493	0.428	0.486	0.500
CA	0.335	0.256	0.324	0.352	0.306
CB	0.383	0.152	0.316	0.198	0.223
CG	0.119	0.175	0.256	0.258	0.151
OD1	−1.042 (−1.105)	−1.171 (−1.120)	−1.104 (−1.098)	−1.209 (−1.106)	−1.237 (−1.132)
OD2	−1.297 (−1.125)	−1.363 (−1.128)	−0.382 (−0.879)	−1.157 (−1.126)	−0.928 (−1.082)
Whole residue	−0.233	−0.316	1.074	0.196	0.251
Backbone	1.605	1.891	1.989	2.106	2.034
Side chain	−1.837	−2.207	−0.915	−1.910	−1.782
—COO^- group	−2.220	−2.359	−1.231	−2.108	−2.015
H-bond	−2.236	−2.258	−1.990	−2.232	−2.222

Notes: Atomic hydrophobicity depends on the host peptide structure, the neighbouring side chain residues and the position of the AA of interest in the host peptide structure. The number in brackets is the H-bond energy component and 'H-bond' is the sum of H-bonding energies of all individual atoms in the whole residue.

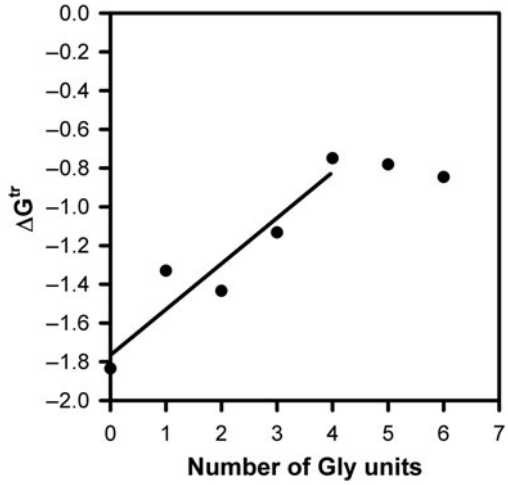

Figure 6. Effect of the amino group NH_2 on the hydrophobicity of the Asp side chain atoms as a function of the number of Gly spacer units. The effect diminishes after 4 Gly residues.

included in Table 3, which show the effects of occlusion of water from the AA backbone atoms in that series. The backbone free energy of transfer in this series had a value between 1.8 and 2.4 kcal mol^{-1}, compared with 1.3–1.8 kcal mol^{-1} for the backbone group in Ac-**X**-NH_2, which experienced much less water occlusion. On the other hand, the Ac-GG-**X**-GG-NH_2 structure tends to expose the side chain atoms of the Asp residue more. A notable difference between the two oxygen atoms in the carboxyl group of Asp in Ac-**D**-GGGG-NH_2 and Ac-**D**-GGGGG-NH_2 is due to the attraction of one of the atoms towards the host backbone, leading to one oxygen atom being more exposed to water, while the other was slightly shielded (in Figure 7(d), the oxygen atom mentioned is indicated by the green arrow). The observed variation of hydrophobicity of the Asp atoms, when this residue was placed at different positions within the sequence of a host peptide (e.g. Ac-**D**-GG-NH_2 compared to Ac-G-**D**-G-NH_2, Table 2), or within host peptide structures flanked by different neighbouring side chain residues (as shown for the exemplars listed in Table 2), demonstrates that the changes in the atomic hydrophobicity arising from structural variation in the chemical environment of the atoms can be calculated by this new method. Similar considerations apply to variations in the type of solvation of individual atoms within a peptide structure. As such, in principle, the full numerical range of intrinsic atomic hydrophobicities associated with structural or solvational changes, e.g. changes in the chemical environment, can be evaluated from the use of this developed simulation approach and associated calculations.

The Phe atoms in Ac-GG-**F**-GG-NH_2 can be used as a further example to illustrate the utility of the HI and atomic free energy of transfer, ΔG^{tr}_{aa}, to define the atomic hydrophobicity. Table 4 shows that the backbone oxygen atom in the Phe residue is the most hydrophobic. Although this finding contradicts the RDF results (Figure 8), which indicated that the backbone oxygen atom is quite hydrophilic in comparison to the other atoms, on closer inspection of the results, it is apparent that its WEDD skews significantly to the right, indicating that there are significant periods of time when water cannot get close to the atom. Moreover, the HI list shows that this atom is relatively occluded from water. Visualisation of the MD trajectory clearly shows that although water can come in close proximity to this oxygen atom for some short periods of time, there are other, more extended periods of time when the atom is shielded from water by the two Gly arms of the host peptide and by the residue side chain ring (Figure 7(e), the oxygen atom is highlighted). The values of the atomic

Table 3. Comparison of HI (*) of Asp atoms in (1) Ac-**D**-NH_2, (2) Ac-WL-**D**-LL-NH_2 and (3) Ac-GG-**D**-GG-NH_2; and HI (*) and atomic free energy of transfer (**) of atoms in selected AA whole residues in series Ac-GG-**X**-GG-NH_2.

Asp				Leu			Glu			Lys			Tyr			Trp		
	(*) (1)	(*) (2)	(*) (3)		(*)	(**)		(*)	(**)		(*)	(**)		(*)	(**)		(*)	(**)
N	0.797	0.991	0.997	**N**	1.087	0.872	N	0.951	0.654	N	0.968	0.639	N	0.695	0.505	N	1.168	0.782
O	0.375	0.806	0.607	O	0.588	0.541	O	0.589	0.464	O	0.570	0.600	O	0.764	0.607	O	0.654	0.568
C	0.593	1.183	0.845	C	0.789	0.446	C	0.772	0.382	C	0.748	0.413	C	0.925	0.517	C	0.774	0.446
CA	0.944	0.860	0.760	CA	1.000	0.450	CA	0.829	0.307	CA	0.874	0.387	CA	0.760	0.359	CA	0.952	0.414
CB	0.568	0.379	0.298	CB	0.797	0.394	CB	0.540	0.332	CB	0.630	0.333	CB	0.562	0.290	CB	0.688	0.377
CG	0.360	0.363	0.295	CG	0.607	0.351	CG	0.277	0.240	CG	0.509	0.269	CG	0.652	0.311	CG	0.802	0.457
OD1	0.226	0.190	0.167	CD1	0.427	0.234	CD	0.320	0.228	CD	0.376	0.306	CD1	0.512	0.279	CD1	0.492	0.281
OD2	0.288	0.317	0.218	CD2	0.464	0.265	OE1	0.202	−1.009	CE	0.252	0.350	CD2	0.563	0.400	CD2	0.951	0.687
							OE2	0.217	−1.115	NZ	0.213	−0.252	CE1	0.360	0.303	CE2	0.642	0.453
													CE2	0.419	0.321	CE3	0.613	0.372
													CZ	0.376	0.341	CZ2	0.392	0.344
													OH	0.228	0.242	CZ3	0.384	0.331
																CH2	0.344	0.347
																NE1	0.470	0.372

Note: The free energy of transfer is expressed in kcal mol^{-1}.

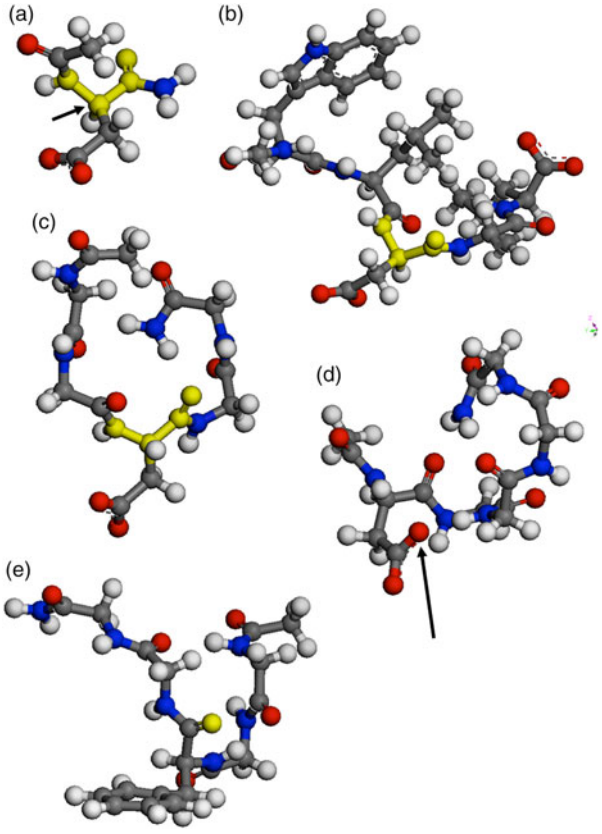

Figure 7. (Colour online) Conformations of selected peptide structures illustrating the behaviour of the AA atoms during MD simulation: (a) Asp CA atom (indicated by the arrow) in Ac-**D**-NH_2 is hindered from surrounding water by the acetyl, amide and Asp side chain atoms, all Asp backbone atoms are highlighted; (b) Asp backbone atoms in Ac-WL-**D**-LL (highlighted) are surrounded by Leu neighbouring side chains; (c) Asp backbone atoms in Ac-GG-**D**-GG-NH_2 (highlighted) are surrounded by the two Gly arms of the host peptide; (d) one carboxyl oxygen atom in Ac-**D**-GGGG-NH_2 (indicated by the arrow) tends to attract more towards the host peptide backbone and (e) the backbone oxygen atom in Ac-GG-**F**-GG-NH_2 (highlighted) is surrounded by the two Gly arms of the host peptide backbone and the Phe side chain ring.

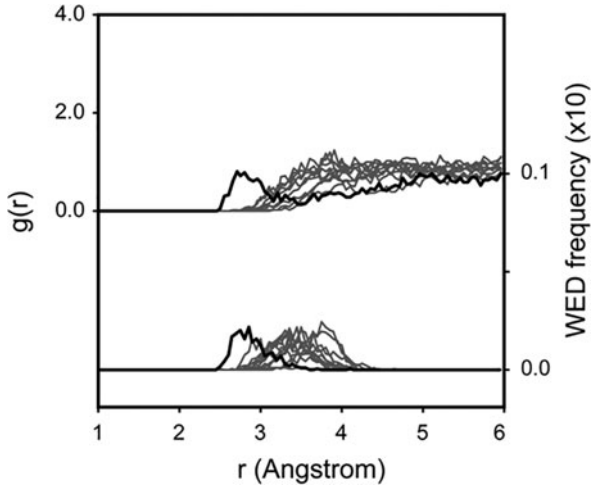

Figure 8. RDFs with respect to water oxygen atoms (upper panel) and WEDD (lower panel) for Phe atoms in Ac-GG-**F**-GG-NH_2. The RDF and WEDD curves of the backbone oxygen atom are shown in black, whereas the curves for all other atoms are in grey. The WED curve has a skewed shape indicating that there are periods of time when water cannot get close to the backbone oxygen atom. The WED curves were normalised and scaled by 10 times for better visualisation.

free energy of transfer and the HI (in Table 4) are very consistent with the MDs simulated behaviour of the peptide.

Also included in Table 4 are values for the average ASA values (for several randomly selected frames in the trajectory) obtained for all of the atoms of the Phe residue using the NACCESS software [45] across the MDs experiment, and the ASA values for the Phe residue in a fully extended conformation as reported in Eisenberg et al. [15] NACESS is a (freeware) computer program, developed by Tsodikov et al. [39] to allow the calculation of accessible and molecular surface areas and average surface curvature for a peptide structure. The ASA values for all atoms in the Phe residue calculated by NACCESS follow a similar trend to those

Table 4. HI, free energy of transfer (kcal mol^{-1}) and time-averaged WED (Å), calculated by this work for Phe atoms in Ac-GG-**F**-GG-NH_2 (columns 2, 3 and 6, respectively).

Phe atoms	HI	Atomic free energy of transfer	ASA (NACCESS)[39]	ASA (Eisenberg et al.)[15]	WED
N	0.90	0.63	11.43	6	3.259
O	1.09	0.80	19.93	24	2.882
C	1.24	0.59	0.144	3	3.760
CA	0.94	0.38	4.311	5	3.726
CB	0.65	0.31	32.02	23	3.555
CG	0.84	0.41	1.708	3	3.630
CD1	0.65	0.49	18.75	23	3.424
CD2	0.60	0.35	21.88	23	3.434
CE1	0.43	0.37	33.14	37	3.334
CE2	0.40	0.35	33.56	37	3.335
CZ	0.37	0.31	9.315	38	3.313

Notes: Average ASA value ($Å^2$) for the Phe atoms for several randomly selected frames across their MD trajectory, calculated by the NACCESS program [45] using radii values from Richmond and Richards [46] (column 4); and ASA ($Å^2$) for the Phe atoms in a fully extended Phe conformation listed in Eisenberg et al. [15] (column 5).

reported by Eisenberg et al. [15] with the exception of the carbon atom in the aromatic ring CZ, probably because the NACCESS ASA value is not appropriate for the peptide's fully extended conformation. As NACCESS measures single-frame ASA values, to determine ASA values for a dynamics trajectory, we used the averaged values of a number of randomly selected frames in the trajectory.

A comparison of the ASA, WED, HI and atomic free energy of transfer calculated from the MD experiments demonstrates the differences among these parameters. Through the use of a commonly employed comparison approach that enabled assessment of the gradient (for magnitude and trend) and the correlation coefficient against literature data, the derived hydrophobicity values were found to fall inside the corresponding ranges reported in the literature.[8,9,13,15,17,19–21] ASA represents the geometrical interface between the solute and water, while the WEDD defines the dynamic interface where the AA atoms exhibit apparent maximum hydrophobicity potential. The HI contains information on the degree of repulsion to water (or exclusion from water) as it is based on the number of water molecules that the AA atom is exposed to at the whole residue interface. On the other hand, the atomic free energy of transfer can be understood as the work required to solvate an individual atom and thus a measure of the atomic hydrophobicity itself. Determination of the atomic free energy of transfer, ΔG^{tr}_{aa}, thus provides a complete measure to quantify the hydrophobicity at the atomic level for each individual atom in the peptide structure. Moreover, participation of intramolecular hydrogen bonds and interactions, as clearly evident in case of the Asp residue in Ac-WL-D-LL and Ac-D-NH_2, would be expected to determine the extent of hydration or exclusion of the atoms of each peptide.

4. Conclusions

In this paper, we describe a new computational approach to estimate the atomic free energy of transfer, ΔG^{tr}_{aa}, and the HI values for each atom in small peptide structures. The free energy of transfer values, ΔG^{tr}_{aa}, for the 20 proteinogenic AAs, as found in N-acetyl AA amides, calculated by this new method agreed well with other published experimental and computational modelling data.

This current study thus demonstrates that

(i) The atomic free energy of transfer can be estimated as a sum of the atom's hydrophobic free energy (ΔE_{aa}) and H-bonding energy,
(ii) The WEDD can be used to delineate the dynamic interface boundary between the atom and surrounding water molecules, where the atom has maximum apparent hydrophobicity potential and
(iii) The use of water molecules in this interface boundary is sufficient for the purpose of estimation of the atom's free energy of transfer, ΔG^{tr}_{aa}.

Collectively, the results from this study confirm that this new method provides a useful and versatile tool to investigate the hydrophobicity of small peptides at the atomic level. At this stage of development, the scope of this new method has been limited to applications with small peptides since extension to larger polypeptides or proteins, with, e.g. more than 50–100 AA residues, where higher order secondary or tertiary domain structures occur, would require more theory development and validation. Nevertheless, since the atomic hydrophobicity can be described as a single number, the method, at its current stage of development, provides a useful approach to map the atomic hydrophobicity of not only small peptide structures in a water environment, but also, in principle, other low-molecular weight organic compounds in a defined solvational environment. Furthermore, as the method measures the relative hydrophobicity of an atom in comparison to the hydrophobicity of other atoms in the same molecular structure under the same simulation condition, it is suitable for implementation for use with any other force field or MDs software.

Acknowledgements

The authors would like to thank Prof Mark E. Tuckerman, New York University, for providing the reference RDF data in Figure 1 and Dr Oleg V. Tsodikov, University of Michigan, for the NACCESS software and his assistance with its use.

Disclosure statement

No potential conflict of interest was reported by the authors.

Funding

This work was financially supported at Monash University by the Commonwealth of Australia through the Australian Research Council and the Department of Industry, Innovation, Science and Research under the International Science Linkages program as part of the Australian-European integrated FP6 project 'Charged particle nanotechnology' (CHARPAN) and FP7 project 'Bio-Inspired Self-assembled Nano-Enabled Surfaces' (BISNES).

Note

1. Current address: Department of Bioengineering, Faculty of Engineering, McGill University, Montreal, Quebec, Canada H3A 0C3

References

[1] Tanford C. The hydrophobic effect: formation of micelles and biological membranes. 2nd ed. New York: Wiley; 1980.
[2] Creighton TE. Proteins. Structure and molecular principles. New York, NY: Freeman; 1984.
[3] Hearn MTW. Conformational behaviour of polypeptides and proteins in reversed phase and lipophilic environments. In: Vijayalakshmi MA, editor. Biochromatography: Theory and Practice. London (UK): Taylor & Francis; 2002. p. 72–141.

[4] Zimmerman JM, Eliezer N, Simha R. The characterization of amino acid sequences in proteins by statistical methods. J Theor Biol. 1968;21:170–201. doi:10.1016/0022-5193(68)90069-6.

[5] Chothia C. The nature of the accessible and buried surfaces in proteins. J Mol Biol. 1976;105:1–12. doi:10.1016/0022-2836(76)90191-1.

[6] Su SJ, Grego B, Niven B, Hearn MTW. Analysis of group retention contributions for peptides separated by reversed phase high performance liquid chromatography. J Liq Chromatogr. 1981;4:1745–1764. doi:10.1080/01483918108064844.

[7] Fauchère JL, Pliska V. Hydrophobic parameters pi of amino acid side chains from the partitioning of *N*-acetyl-amino acid amides. Eur J Med Chem. 1983;18:369–375.

[8] Wilce MCJ, Aguilar M-I, Hearn MTW. Physicochemical basis of amino acid hydrophobicity scales: evaluation of four new scales of amino acid hydrophobicity coefficients derived from RP-HPLC of peptides. Anal Chem. 1995;67:1210–1219. doi:10.1021/ac00103a012.

[9] Mannhold R, Rekker RF. The hydrophobic fragmental constant approach for calculating log *P* in octanol/water and aliphatic hydrocarbon/water systems. Perspect Drug Discov Design. 2000;18:1–18. doi:10.1023/A:1008782809845.

[10] Aliste MP, Tieleman DP. Computer simulation of partitioning of ten pentapeptides Ace-WLXLL at the cyclohexane/water and phospholipid/water interfaces. BMC Biochem. 2005;6:30, 1–15. doi:10.1186/1471-2091-6-30.

[11] Honciuc A, Baptiste DJ, Schwartz DK. Hydrophobic interaction microscopy: mapping the solid/ liquid interface using amphiphilic probe molecules. Langmuir. 2009;25:4339–4342. doi:10.1021/la9004246.

[12] Sarkar A, Kellogg GE. Hydrophobicity-shake flasks, protein folding and drug discovery. Curr Topics Med Chem. 2010;10:67–83. doi:10.2174/156802610790232233.

[13] Abraham DJ, Leo AJ. Extension of the fragment method to calculate amino acid zwitterion and side chain partition coefficients. Prot Struct Funct Genet. 1987;2:130–152. doi:10.1002/prot.340020207.

[14] Eisenberg D, McLachlan AD. Solvation energy in protein folding and binding. Nature. 1986;319:199–203. doi:10.1038/319199a0.

[15] Eisenberg D, Wesson M, Yamashita M. Interpretation of protein folding and binding with atomic solvation parameters. Chem Scr. 1989;29A:217–221, 211 plate.

[16] Abraham DJ, Kellogg GE. The effect of physical organic properties on hydrophobic fields. J Comput Aided Mol Des. 1994;8:41–49. doi:10.1007/BF00124348.

[17] Wimley WC, Creamer TP, White SH. Solvation energies of amino acid side chains and backbone in a family of host–guest pentapeptides. Biochemistry. 1996;35:5109–5124. doi:10.1021/bi9600153.

[18] Wimley WC, White SH. Experimentally determined hydrophobicity scale for proteins at membrane interfaces. Nat Struct Biol. 1996;3:842–848. doi:10.1038/nsb1096-842.

[19] Mannhold R, Poda GI, Ostermann C, Tetko IV. Calculation of molecular lipophilicity: state-of-the-art and comparison of log *P* methods on more than 96,000 compounds. J Pharm Sci. 2009;98:861–893. doi:10.1002/jps.21494.

[20] Shrake A, Rupley JA. Environment and exposure to solvent of protein atoms. Lysozyme and insulin. J Mol Biol. 1973;79:351–371. doi:10.1016/0022-2836(73)90011-9.

[21] Chothia C. Hydrophobic bonding and accessible surface area in proteins. Nature. 1974;248:338–339. doi:10.1038/248338a0.

[22] Durchschlag H, Zipper P. Volume, surface and hydration properties of proteins. Progr Coll Polym Sci. 2008;134:19–29.

[23] Plazzer MB, Henry DJ, Yiapanis G, Yarovsky I. Comparative study of commonly used molecular dynamics force fields for modeling organic monolayers on water. J Phys Chem B. 2011;115:3964–3971. doi:10.1021/jp1116867.

[24] Künzel D, Groß A. Influence of the solvent on the stability of bis(terpyridine) structures on graphite. Beilstein J Nanotechnol. 2013;4:269–277. doi:10.3762/bjnano.4.29.

[25] Oguike RS, Oni O. Computational simulation and inhibitive properties of amino acids for mild steel corrosion: adsorption in gas phase onto Fe (110). Int J Res Chem Environ. 2014;4:177–186.

[26] Kabsch W. A discussion of the solution for the best rotation to relate two sets of vectors. Acta Cryst Acta Cryst. 1978;A34:827–828. doi:10.1107/S0567739478001680.

[27] Ho BK, Dill KA. Folding very short peptides using molecular dynamics. PLoS Comput Biol. 2006;2:228–237.

[28] Mancera RL, Buckingham AD. Molecular properties of and temperature effects on the hydrophobic hydration of ethane. J Phys Chem. 1995;99:14632–14640. doi:10.1021/j100040a010.

[29] Mancera RL. Towards an understanding of the molecular basis of hydrophobicity. J Comput Aided Mol Des. 1996;10:321–326. doi:10.1007/BF00124501.

[30] Held M, Nicolau DV. Estimation of atomic hydrophobicities using molecular dynamics simulation of peptides. Proc SPIE. 2008;6799:679916/679911–679916/679917.

[31] Widom B. Statistical mechanics: a concise introduction for chemists. Cambridge: Cambridge University Press; 2002.

[32] Pace CN, Shirley BA, McNutt M, Gajiwala K. Forces contributing to the conformational stability of proteins. FASEB J. 1996;10:75–83.

[33] Lee H-S, Tuckerman ME. Structure of liquid water at ambient temperature from *ab initio* molecular dynamics performed in the complete basis set limit. J Chem Phys. 2006;125:154507/154501–154507/154514.

[34] Soper AK. The radial distribution functions of water and ice from 220 to 673 K and at pressures up to 400 MPa. Chem Phys. 2000;258:121–137. doi:10.1016/S0301-0104(00)00179-8.

[35] Hura G, Sorenson JM, Glaeser RM, Head-Gordon T. A high-quality X-ray scattering experiment on liquid water at ambient conditions. J Chem Phys. 2000;113:9140–9148. doi:10.1063/1.1319614.

[36] Luise A, Falconi M, Desideri A. Molecular dynamics simulation of solvated azurin: correlation between surface solvent accessibility and water residence times. Prot Struct Funct Genet. 2000;39:56–67. doi:10.1002/(SICI)1097-0134(20000401)39:1<56:AID-PROT6>3.0.CO;2-5.

[37] Bandyopadhyay S, Chakraborty S, Balasubramanian S, Bagchi B. Sensitivity of polar solvation dynamics to the secondary structures of aqueous proteins and the role of surface exposure of the probe. J Am Chem Soc. 2005;127:4071–4075. doi:10.1021/ja042847r.

[38] Nguyen MT, Chaffee AL, Held M, Boysen RI, Nicolau DV, Hearn MTW. A study on the atomic hydrophobicity of peptides in aqueous solutions using molecular dynamics modeling methods. Proc SPIE. 2008;6799:679916–679912.

[39] Fauchère JL, Quarendon P, Kaetterer L. Estimating and representing hydrophobicity potential. J Mol Graph. 1988;6:203–206, 202. doi:10.1016/S0263-7855(98)80004-0.

[40] Kellogg GE, Semus SF, Abraham DJ. HINT: a new method of empirical hydrophobic field calculation for CoMFA. J Comput Aided Mol Des. 1991;5:545–552. doi:10.1007/BF00135313.

[41] Lee B, Richards FM. The interpretation of protein structures: estimation of static accessibility. J Mol Biol. 1971;55:379–400. doi:10.1016/0022-2836(71)90324-X.

[42] Connolly ML. Solvent-accessible surfaces of proteins and nucleic acids. Science. 1983;221:709–713. doi:10.1126/science.6879170.

[43] Richmond TJ. Solvent accessible surface area and excluded volume in proteins: Analytical equations for overlapping spheres and implications for the hydrophobic effect. J Mol Biol. 1984;178:63–89. doi:10.1016/0022-2836(84)90231-6.

[44] Muller N. Search for a realistic view of hydrophobic effects. Acc Chem Res. 1990;23:23–28. doi:10.1021/ar00169a005.

[45] Tsodikov OV, Record MT Jr., Sergeev YV. Novel computer program for fast exact calculation of accessible and molecular surface areas and average surface curvature. J Comput Chem. 2002;23:600–609. doi:10.1002/jcc.10061.

[46] Richmond TJ, Richards FM. Packing of α-helices: geometrical constraints and contact areas. J Mol Biol. 1978;119:537–555. doi:10.1016/0022-2836(78)90201-2.